Real-time Multiple Abnormality Detection in Video Data

Have, Simon Hartmann; Ren, Huamin; Moeslund, Thomas B.

Published in:
INSTICC

Publication date:
2013

Document Version
Accepted author manuscript, peer reviewed version

Real-time Multiple Abnormality Detection in Video Data

Simon Hartmann Have, Huamin Ren and Thomas B. Moeslund
Visual Analysis of People Lab, Aalborg University, Denmark
hr@create.aau.dk

Keywords: Abnormality detection; Cascade classifier; Video surveillance; Optical flow.

Abstract: Automatic abnormality detection in video sequences has recently gained an increasing attention within the research community. Although progress has been seen, there are still some limitations in current research. While most systems are designed at detecting specific abnormality, others which are capable of detecting more than two types of abnormalities rely on heavy computation. Therefore, we provide a framework for detecting abnormalities in video surveillance by using multiple features and cascade classifiers, yet achieve above real-time processing speed. Experimental results on two datasets show that the proposed framework can reliably detect abnormalities in the video sequence, outperforming the current state-of-the-art methods.

1 INTRODUCTION

Abnormality detection is an important problem that has been researched within diverse research areas and application domains. Many abnormality detection techniques have been specially developed for certain application domains, e.g. car counting (Stauffer and Grimson, 2000), group activity detection (Cui et al., 2011), monitoring vehicles (Yu and Medioni, 2009) etc. A key issue when designing an abnormality detector is how to represent the data in which anomalies are to be found. Considering approaches in the context of video surveillance, existing methods in the literature can be classified into two categories:

1) Data analysis by tracking, in which objects are represented by trajectories. A commonly used approach is based on obtained clusters of the trajectories for moving objects, which are later used as an abnormality model. Johnson et al. (Johnson and Hogg, 1995) were probably among the first researches in this direction, they used vector quantization to obtain a compact representation of trajectories and utilized multilayer neural networks for the identification of common patterns. Piciarelli et al. (Piciarelli and Foresti, 2006) proposed a trajectory clustering algorithm especially suited for online abnormality detection. Hu et al. (Hu et al., 2006) hierarchically clustered trajectories depending on spatial and temporal information. While trajectory based approaches are suitable in scenes with few objects, they cannot maintain reliable tracks in crowded environments due to occlusion and overlap of objects (Mahadevan et al., 2010).

2) Data analysis without tracking, in which features such as motion or texture are extracted to model activity patterns of a given scene. Different features have been attempted. For example, Mehran et al. (Mehran et al., 2009) modeled crowd behavior using a "social force" model, where the interaction forces were computed using optical flow. (Mahadevan et al., 2010) recently proposed mixtures of dynamic textures to jointly model the appearance and dynamics of crowded scenes, to address the problem of abnormality detection with size or appearance variation in objects. (Zhao et al., 2011) provided a framework of using sparse coding and online re-constructibility to detect unusual events in videos.

Although progress has been made, there are still some limitations in current research: while most systems are designed at detecting specific abnormality, others which are capable of detecting more than two types of abnormalities rely on heavy computation. In this work, we provide a framework of using multiple features and cascade classifiers to detect several abnormal activities in videos yet achieve real-time processing speed.

2 PROPOSED METHOD

Two important criteria to evaluate abnormality detection systems are time response and types of abnormalities that can be detected. To meet the requirements of a practical abnormality detection system, our

system is designed to detect multiple unusual events. To attain this goal, we adopt four types of features, train their corresponding classifiers, and cascade these classifiers to determine if the query video contains abnormality or not.

2.1 System Overview

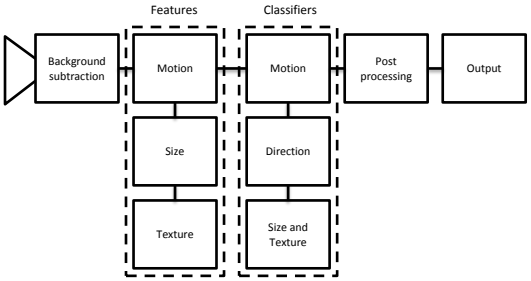

Figure 1: Overview of the system.

An overview of our system is illustrated in Figure 1. A figure-ground segmentation is carried out to extract foreground pixels. This not only allows for using object size as a feature, but also reduces the aperture problem related to image motion detection via optical flow. Foreground segmentation method (Li et al., 2003) is adopted in this paper for the consideration of computational cost. Then, three different features - motion, size and texture - are extracted, where motion is split into two sub-features, namely amount of motion and direction. Next, classifiers are trained to detect multiple abnormalities, including motion, out of place objects and directional abnormal activities. Finally, to minimize the effect of noise, post-processing is introduced, which smooth abnormalities over time, which is based on an easy understood assumption that abnormal behaviors should last for multiple frames due to time consistency.

2.2 Feature Extraction

Every input frame is first divided into equal sized and quadratic regions, then features (motion, size, texture and direction features) are extracted in each region.

Motion Feature: Optical flow represents apparent motion of the object relative to the observer. Three different approaches for estimating optical flow are here considered: Lucas-Kanade (Lucas and Kanade, 1981), Pyramid Lucas-Kanade (Bouguet, 2000) and Horn-Schunck (Horn and Schunck, 1981). Both Lucas-Kanade approaches are local method that operate on small regions to obtain the optical flow. Horn-Schunk on the other hand operates as a global method that uses the global smoothness to compute optical flow. The flow is calculated on each pixel using these three methods. Note that we only use foreground pixels to represent the feature. This makes the estimations more stable:

$$\hat{mot}_t(i,j) = \frac{1}{N_f} \sum_{n=0}^{N_f} \parallel [v_x^{(n)}, v_y^{(n)}]_1 \parallel \tag{1}$$

where for each foreground pixel n, $v_x^{(n)}$ and $v_y^{(n)}$ are the optical flow in both spatial directions and N_f is the total number of foreground pixels.

To further reduce the effect of noise, the motion feature for a region is averaged by the motion features in the same region of the neighboring frames $t-1$ and $t+1$:

$$mot_t(i,j) = \frac{1}{3} \sum_{u=t-1}^{t+1} \hat{mot}_u(i,j) \tag{2}$$

Pyramid Lucas-Kanade is a spares method and the average motion will therefore not be normalized based on foreground pixels, but rather based on the number of flow vectors within the region:

$$\hat{mot}_t(i,j) = \frac{1}{N_{fv}} \sum_{n=0}^{N_f} \parallel [v_x^{(n)}, v_y^{(n)}]_1 \parallel \tag{3}$$

where for each optical flow vector n, $v_x^{(n)}$ and $v_y^{(n)}$ are the optical flow in both spatial directions and N_{fv} is the total number of flow vectors within the region.

Size Feature: Size feature is based on the occupancy of the foreground pixels in each region combined with occupancy in its neighboring regions. Neighboring regions in the current frame are used since the object might fill up more than one region. A Gaussian kernel is used to put more emphasis on the current calculated region and less emphasis on its neighborhood.

$$size_t(i,j) = \sum_{a=i-1}^{i+1} \sum_{b=j-1}^{j+1} G(a-i+1, b-j+1) o_t(a,b) \tag{4}$$

where G is a 3x3 Gaussian kernel and o_t is the occupancy map of the region.

Texture Feature: For the texture feature we apply the magnitude of the output of a 2D Gabor filter. In this work we use wavelets in four directions: 0° , 45°, 90° and 135°. To avoid modeling the background, the texture feature is only extracted for regions that have foreground pixels. The following definition of the Gabor filter is used in this work (Lee, 1996):

$$G(x;y;\omega;\theta) = \frac{\omega}{\sqrt{2\pi}K} e^{-\frac{\omega^2}{8K^2}(4x'^2+y'^2)} [\cos(\omega x') - e^{\frac{-k^2}{2}}] \tag{5}$$

where $x' = x\cos\theta + y\sin\theta$, $y' = -x\sin\theta + y\cos\theta$, ω is the radial frequency of the filter, θ specifies the orientation and K is the frequency bandwidth. The resulting vector for the texture feature is given as:

$$txt_t(i,j) = [m_0 \;\; m_{45} \;\; m_{90} \;\; m_{135}] \tag{6}$$

Direction Feature: The direction feature is here defined as a four bin histogram containing the directions of the optical flow vectors estimated in motion feature. For each pixel in the foreground, its optical flow values are converted to an angle $\Theta \in [0°, 359°]$:

$$\Theta = atan2(\frac{dy}{dt}, \frac{dx}{dt}) \tag{7}$$

The directions are quantified into four bin, as illustrated below:

- Bin 1: $[45° : 135°[$;
- Bin 2: $[135° : 225°[$;
- Bin 3: $[225° : 315°[$;
- Bin 4: $[315° : 360°[$ and $[0° : 45°[$.

The resulting output vector is given as:

$$dir_t(i,j) = [b_1 \;\; b_2 \;\; b_3 \;\; b_4] \tag{8}$$

where b_1 is the first bin etc.

2.3 Classifiers

There are four classifiers, which work in a cascade. First, the classifier for motion is executed, if no abnormality detected, the classifier for size and texture are combined to determine an abnormality. This is because size alone does not necessarily constitute an abnormality, e.g. a group of people standing close. The direction classifier works independently to detect direction abnormality.

Different classifiers are adopted to deal with different features. For motion and size features, classifiers are trained offline by finding motion/size features in each frame in a training set. This ends up with a histogram, which is then smoothed, discretized and normalized to obtain a probability mass function (pmf). A region is recognized as abnormal if its pmf of motion and size satisfies the following two equations:

$$pmf_{mot}(mot_t(i,j)) < T_{motion} \tag{9}$$

$$pmf_{size}(size_t(i,j)) < T_{size} \tag{10}$$

where T is a decision threshold.

The classifier for the texture feature is based on an adaptive codebook. The main idea is to calculate the distance between input features with the entries in the codebook (also called codewords) to find possible abnormalities. Considering the ability to normalize texture contrast variations, we use Pearson's correlation coefficient (Boslaugh and Watters, 2008) as a distance measure. To train the classifier, the first 4D texture descriptor in each region is taken as the first entry. Then for each new texture feature we measure the similarity by Pearson's correlation coefficient:

$$p(a,b) = \frac{(a-\mu_a)\cdot(b-\mu_b)}{\| a-\mu_a \| \| b-\mu_b \|} \tag{11}$$

where μ_x is the mean of vector x and $p(a,b)$ is in the interval $[-1,1]$.

The output of the classifier is normality if the distance between the input vector and all the entries in the codebook are all larger than a predefined threshold (0.9 in this work). In that case, the codeword with the highest correlation coefficient is updated as in equation 12; otherwise, the input is added as an entry to the codebook and the output of the classifier is abnormality.

$$c_k^{new} = c_k^{old} + \frac{1}{W_k + 1}(x_{in} - c_k^{old}) \tag{12}$$

where c_k is the best matching codebook entry, W_k is the number of vectors so far assigned to the codebook entry k and x_{in} is the input descriptor.

A simple classifier is trained for the directional feature in order to keep the processing down. We average over the directional features during training and then normalizing the resulting vector to 1. A newly incoming direction feature is first normalized and then compared to the trained model by simple element-wise subtraction. The sum of the absolute values of the four subtractions is compared with a threshold and judged as an abnormality if it surpassed the threshold:

$$v_{direction} = \sum \left| \begin{bmatrix} h_1 \\ h_2 \\ h_3 \\ h_4 \end{bmatrix} - \begin{bmatrix} x_1 \\ x_2 \\ x_3 \\ x_4 \end{bmatrix} \right| \tag{13}$$

where h is the normalized classifier vector and x is the normalized incoming direction feature vector.

3 EXPERIMENTAL RESULTS

3.1 Datasets

To test the motion, size and texture features and classifiers, the UCSD anomaly detection dataset (ucs, 2008) is used, which is a public dataset for anormality detection. The UCSD dataset consists of two subsets, Ped1 and Ped2, both having training and testing parts. Classifiers are trained and testing frames

containing one or more abnormal features are defined as abnormalities which are later compared with the ground truth.

To detect direction abnormality, we obtain hours of traffic cam footage from a highway in Maryland, recorded from (mar, 2012). The refresh rate is 5fps which is sufficient for optical flow given the motion in the testset. To get more direction abnormalities, we edit an hour long video sequence and reverse 15 small sections to simulate cars driving in the wrong direction. The abnormalities are distributed randomly over the entire video. The length of each sequence spans from 25 frames (5 sec) to 125 frames (25 sec). Representative frames in these two datasets are shown in Figure 2.

3.2 Parameter Tuning

We first tune the texture parameters, then change the threshold T_{size} to find normalities and abnormalities in the datasets. Similar to other works, we use False Positive Rate (FPR) and False Negative Rate (FNR) to quantify the results. From experimental investigations, the kernel size is set to approximately half of the standard region size to get symmetric responses on each side of the pixels. The radial frequency ω is set to 2.3 and the frequency bandwidth K is set to π. The only parameter that will be changed is the threshold T_{size} which regulates when a size is found to be abnormal or not. The region size is set to 16 x 16 since the results are quite similar for all three optical flow methods while varying the region size.

3.3 Choice of Optical Flow Method

The search window size for the optical flow is set to 15 x 15 pixels in the Lucas-Kanade based methods, with three pyramid levels and 1000 foreground features in Pyramid Lucas-Kanade. For Horn-Schunck method the stop iteration criteria has been set to 20. The three optical flow methods are tested with different possible thresholds yielding the curves in figure 3 and 4 for the Ped1 and Directional datasets, respectively. As can be seen, Pyramid Lucas-Kanade outperforms the other two methods. This is primarily due to the utilization of "good features to track" that finds structures with a high level of texture that in turn reduces the aperture problem.

3.4 Results

We test our system and compare the results with other methods that test on the UCSD dataset. These are: "Reddy" (Reddy et al., 2011) , "Social Force"

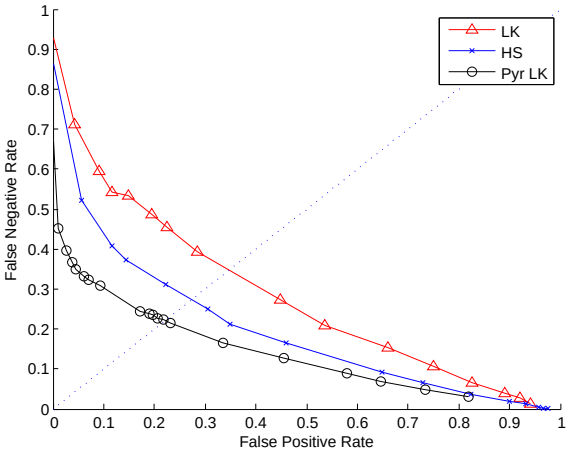

Figure 3: Curve for Pyramid Lucas-Kanade, Lucas-Kanade and Horn-Schunck at 20 histogram bins and region size of 16 x 16. Test dateset: Ped1.

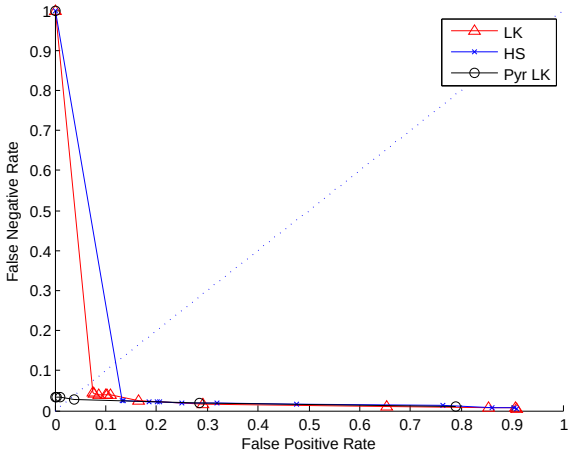

Figure 4: Curve for Pyramid Lucas-Kanade, Lucas-Kanade and Horn-Schunck at 20 histogram bins and region size of 16 x 16. Test dateset: Directional.

(Mehran et al., 2009) , "MDT" (Mahadevan et al., 2010) and "MPPCA" (Kim and Grauman, 2009). The results at frame level are shown in Figure 5 and 6. Moreover we compare abnormality results at pixel level, see Figure 7.

We further calculate the Equal Error Rate (EER) for frame level and pixel level abnormality detection, respectively, see Table 1 and 2. It can be seen in both the figures and tables that our method outperforms other methods in frame level abnormality and for pixel level abnormality detection, the proposed method performs as good as the best of the other methods.

For the direction abnormalities we test on our own dataset as explained above. The results are shown in Figure 8 for two different strategies for direction vec-

a) A representative training frame in UCSD.

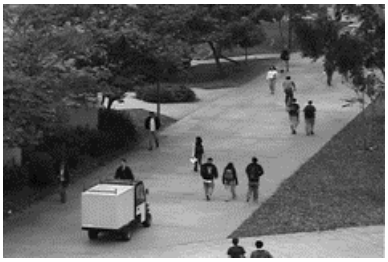

b) A representative testing frame with abnormality: golf car.

c) A representative frame from the direction dataset.

Figure 2: Representative frames from two datasets.

Table 1: EER for frame level abnormality detection on Ped1 and Ped2 subsets of UCSD.

Approach	Social Force	MPPCA	MDT	Reddy	Proposed method
Ped1	31.0%	40.0%	25.0%	22.5%	**20.0%**
Ped2	42.0%	30.0%	25.0%	20.0%	**15.0%**
Average	37.0%	35.0%	25.0%	21.2%	**17.5%**

Table 2: EER for pixel level abnormality detection on Ped1 and Ped2 subsets of UCSD.

Approach	Social Force	MPPCA	MDT	Reddy	Proposed method
Ped1	79.0%	82.0%	55.0%	32.0%	**31.0%**
Ped2	-	-	-	-	**21.0%**

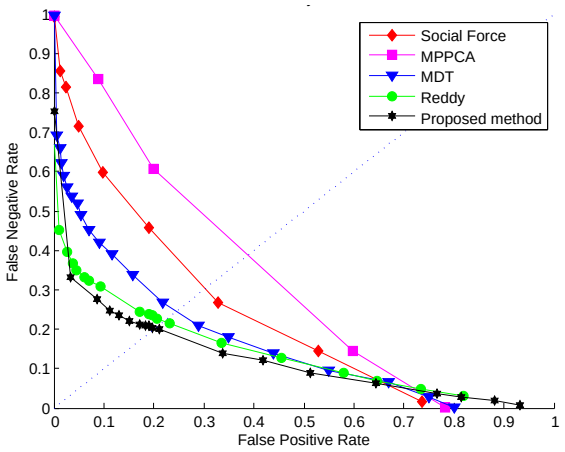

Figure 5: Frame level abnormality detection on Ped1.

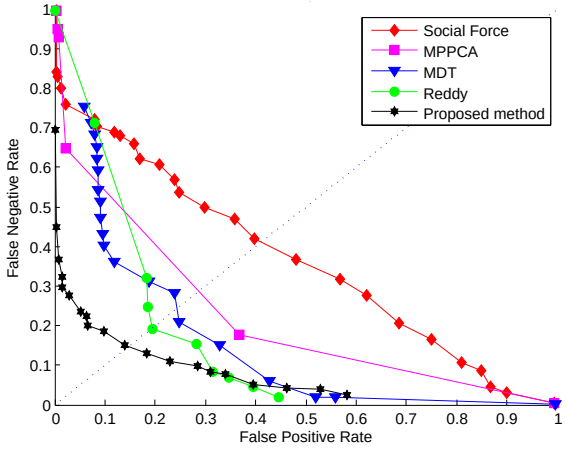

Figure 6: Frame level abnormality detection on Ped2.

tor updating. When computing the four dimensional vector for direction feature, we can increase the direction bin by one or adding the gradient to the direction bin, see results in Figure 8. The difference between the single increment and the gradient increment of the motion seems to be negligible. The total error rate is 0.3%.

At last, we show the computational requirements for the different features. All tests are conducted on an ASUS U46S with an Intel Core i5-2410M CPU running at 2.30 GHz and are calculated with an average FPS in an entire test sequence run. As seen from Table 3, the system is able to work even faster than real-time.

4 CONCLUSIONS

We propose a framework to detect multiple abnormalities in video surveillance, in which motion, size, texture, with direction features are used to train independent classifiers. Experiments show improvements compared to related work. This result is partly caused by less abnormalities in size and texture compared to

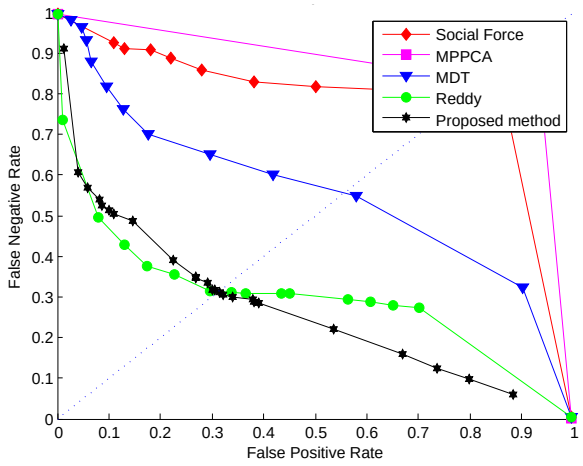

Figure 7: Pixel level abnormality detection on Ped1.

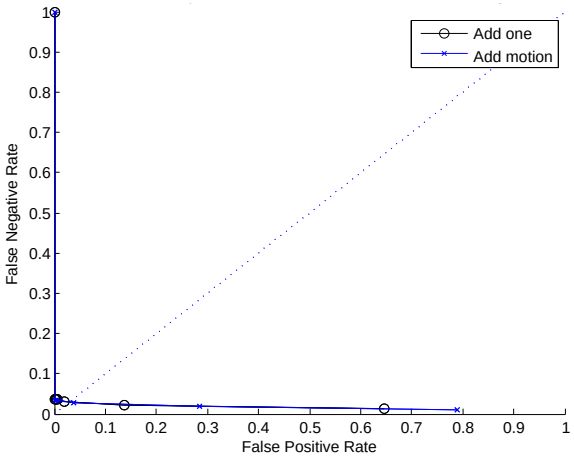

Figure 8: Frame level abnormality detection on the directional dataset, with the two different updating methods.

motion abnormalities in the datasets. Equally importantly, our proposed system is able to run faster than real-time, which allows for connecting four or five cameras to a single computer.

Table 3: Datasets with their respective FPS using different features.

	Ped1	Ped2	Direction
Size	238 x158	360 x240	320 x240
Motion FPS	50	40	-
Size/Texture FPS	20	15	
Motion & Size /Texture FPS	18	12	-
Direction FPS			50

REFERENCES

(2008). Ucsd anomaly dataset. `http://www.svcl.ucsd.edu/projects/anomaly/dataset.html`.

(2012). Maryland department of transportation. `http://www.traffic.md.gov/`.

Boslaugh, S. and Watters, P. (2008). *Statistics in a Nutshell*. O'Reilly Media, Inc.

Bouguet, J. (2000). Pyramidal implementation of the lucas kanade feature tracker description of the algorithm.

Cui, X., Liu, Q., Gao, M., and Metaxas, D. (2011). Abnormal detection using interaction energy potentials. In *CVPR*.

Horn, B. and Schunck, B. (1981). Determining optical flow. *Artificial Intelligence*.

Hu, W., Xiao, X., Fu, Z., Xie, D., Tan, T., and Maybank, S. (2006). A system for learning statistical motion patterns. *PAMI*.

Johnson, N. and Hogg, D. (1995). Learning the distribution of object trajectories for event recognition. In *British conference on Machine vision*.

Kim, J. and Grauman, K. (2009). Observe locally, infer globally: A space-time mrf for detecting abnormal activities with incremental updates. In *CVPR*.

Lee, T. (1996). Image representation using 2d gabor wavelets. *PAMI*, 18:959–971.

Li, L., W. Huang, I. G., and Tian, Q. (2003). Foreground object detection from videos containing complex background. In *ACM international conference on Multimedia*.

Lucas, B. and Kanade, T. (1981). An iterative image registration technique with an application to stereo vision. In *International joint conference on Artificial intelligence*.

Mahadevan, V., Li, W., Bhalodia, V., and Vasconcelos, N. (2010). Anomaly detection in crowded scenes. In *CVPR*.

Mehran, R., Oyama, A., and Shah, M. (2009). Abnormal crowd behavior detection using social force model. In *CVPR*.

Piciarelli, C. and Foresti, G. L. (2006). On-line trajectory clustering for anomalous events detection. *Pattern Recognition Letters*, 27(15):1835–1842.

Reddy, V., Sanderson, C., and Lovell, B. (2011). Improved anomaly detection in crowded scenes via cell-based analysis foreground speed, size and texture. In *International Workshop on Machine Learning for Vision-based Motion Analysis (CVPRW)*.

Stauffer, C. and Grimson, W. (2000). Learning patterns of activity using real-time tracking. *PAMI*, 22(8):747–757.

Yu, Q. and Medioni, G. (2009). Motion pattern interpretation and detection for tracking moving vehicles in airborne video. In *CVPR*.

Zhao, B., Li, F., and Xing, E. (2011). Online detection of unusual events in videos via dynamic sparse coding. In *CVPR*.